

MODE INTERACTIONS IN SCALAR FIELD COSMOLOGY

SPIROS COTSAKIS^{1,2*} AND IGNATIOS ANTONIADIS^{3,4†‡}

¹Clare Hall, University of Cambridge,

Herschel Road, Cambridge CB3 9AL, United Kingdom

²Institute of Gravitation and Cosmology, RUDN University

ul. Miklukho-Maklaya 6, Moscow 117198, Russia

³Institute for Advanced Study

1 Einstein Drive, Princeton, New Jersey 08540, USA

⁴High Energy Physics Research Unit, Faculty of Science

Chulalongkorn University

Phayathai Road, Pathumwan, Bangkok 10330, Thailand

December 2025

*skot@aegean.gr

†antoniad@lpthe.jussieu.fr

‡On leave from LPTHE, Sorbonne Université, CNRS, 4 Place Jussieu, 75005 Paris, France

Abstract

We study the dynamics of spatially homogeneous Friedmann–Robertson–Walker universes filled with a massive scalar field in a neighbourhood of the massless transition $s = 1$. At this point the Einstein–scalar system exhibits a codimension–two Hopf–steady–state organising centre whose versal unfolding describes all small deformations of the quadratic model. After reduction to the centre manifold, the dynamics is governed by two slow geometric modes (r, z) : the Hopf amplitude r , measuring the kinetic departure from de Sitter, and the slowly drifting Hubble mode z . We show that the standard slow–roll parameters follow directly from these unfolding variables, $\epsilon \sim \frac{3}{2}r^2$ and $\eta \sim z$, so that the spectral tilt, tensor–to–scalar ratio, and scalar amplitude arise as universal functions of (r, z) , independently of the choice of potential. The two unfolding parameters (μ_1, μ_2) classify all perturbations of the quadratic model and can be interpreted physically as controlling the tilt and curvature deformations of generic polynomial inflationary potentials. Thus the near scale–invariance of primordial perturbations emerges as a structural property of the unfolding of the organising centre, providing a potential–independent mechanism for an early phase of accelerated expansion. We discuss the implications of this geometric framework for the interpretation and classification of inflationary models.

Contents

1	Introduction	4
2	Summary of the main results	7
3	The versal family: Dynamics and bifurcations	10
3.1	The normal form and versal unfolding	10
3.2	Versal unfoldings and bifurcation structure	12
3.3	Structure of the bifurcation diagrams	13
3.4	Fixed branches and bifurcations	14
4	Physical implications of the versal unfolding	16
4.1	Interpretation of the strata	16
4.2	Implications for the full three-dimensional system	17
4.3	Slow-roll observables from the unfolding	19
4.3.1	Physical meaning of the unfolding parameters	22
5	Discussion	22
	Acknowledgments	24
	References	25

1 Introduction

Scalar fields play a central role in early–universe cosmology, both as effective matter sources within general relativity and as carriers of dynamical degrees of freedom arising from particle physics or modified gravity [1, 2, 3]. In the Friedmann–Robertson–Walker (FRW) setting, the Einstein–scalar equations form a finite-dimensional dynamical system whose qualitative properties can be studied using the tools of bifurcation and singularity theory. This viewpoint is part of a broader programme in which geometrical transitions in GR are interpreted as bifurcations of the underlying field equations [4, 5, 6, 7, 8].

In this paper we revisit the simplest scalar–field cosmology, the FRW universe with a quadratic potential, focusing on the behaviour near the *massless transition*. Although the original chaotic inflation model is disfavoured by current observational constraints [9], various polynomial extensions of it (for example $V \sim \frac{1}{2}m^2\phi^2 + \lambda\phi^n$, $n \in \mathbb{Z}_{>0}$) remain compatible with the cosmic microwave background data (see also [10, 11] for other two-parameter extensions). Our goal is not to advocate a particular potential; rather, we show that the *universal deformation* structure of the Einstein–scalar dynamics near a nondegenerate vacuum already contains the geometric origin of inflationary observables. Pure exponential potentials, which have no stationary point and only scaling solutions, lie in a different universality class and are therefore not covered by the present analysis.

We work with an m –independent scaling of the Einstein–scalar FRW equations, introducing the structural parameter $s = m^2$ as a distinguished control parameter. The resulting system (Eqs. (2.1)–(2.4)) is smooth in s and admits a codimension–two organising centre at $s = 1$ (corresponding to the massless threshold in the original variables). At this point one real and two imaginary eigenvalues become simultaneously neutral, producing a Hopf–steady–state mode interaction. The versal unfolding of this degeneracy yields two canonical families (Cases I and II), organised by saddle–node, pitchfork and Hopf bifurcations, and in the cubic family gives rise to invariant tori describing persistent coupled oscillations of the scalar and geometric modes.

The key result of the paper is that the slow geometric variables of the versal unfolding

provide a direct route to inflationary observables. On the centre manifold the dynamics admits a natural fast–slow decomposition: a fast Hopf phase θ and two slow variables (r, z) , where the Hopf amplitude r measures the kinetic departure from de Sitter while the slow Hubble mode z governs the geometric drift. We show in Sect. 4.4.3 that the Hubble slow–roll parameters satisfy $\epsilon \sim \frac{3}{2}r^2$ and $\eta \sim z$, implying that the spectral tilt, tensor amplitude and scalar power are universal functions of the unfolding coordinates (r, z) and of the deformation parameters (μ_1, μ_2) . For any analytic potential with a nondegenerate vacuum the physical parameters of the model map to (μ_1, μ_2) ; familiar deformations that control tilt and plateau behaviour are thus realised as coordinates on this canonical unfolding, rather than being tied to any particular choice of potential.

The paper is organised as follows. In Sect. 2 we formulate the Einstein–scalar FRW system in m –independent variables and identify the organising centre at $s = 1$. Sect. 3 constructs the Hopf–steady–state normal form and its versal unfoldings, and derives the bifurcation diagrams for Cases I and II. Sect. 4 interprets these structures cosmologically, including the appearance of invariant tori and the universal relations for inflationary observables. We conclude in Sect. 5 with a discussion of the geometric origin of inflation and the role of versal deformations in classifying inflationary models.

What is known about this problem. We consider an FRW universe with curvature index $k = 0, \pm 1$, sourced by a scalar field ϕ with energy density and pressure

$$\rho = \frac{1}{2}\dot{\phi}^2 + V(\phi), \quad p = \frac{1}{2}\dot{\phi}^2 - V(\phi), \quad (1.1)$$

and with the classical massive potential

$$V(\phi) = \frac{1}{2}m^2\phi^2. \quad (1.2)$$

The Einstein–scalar system is then governed by the evolution equations (a dot denotes differentiation with respect to proper time and throughout we work in reduced Planck units $M_{\text{Pl}} = 1$),

$$\ddot{\phi} + 3H\dot{\phi} + m^2\phi = 0, \quad (1.3)$$

$$\dot{H} + H^2 = \frac{1}{6}m^2\phi^2 - \frac{1}{3}\dot{\phi}^2, \quad (1.4)$$

together with the Friedmann constraint

$$H^2 + \frac{k}{a^2} = \frac{1}{6} \left(\dot{\phi}^2 + m^2 \phi^2 \right). \quad (1.5)$$

Classically, the transformation introduced in Refs. [12, 13, 14, 15] rescales the variables using the mass parameter m ,

$$x = \frac{\phi}{\sqrt{6}}, \quad y = \frac{\dot{\phi}}{\sqrt{6}m}, \quad z = \frac{H}{m}, \quad \tau = mt, \quad (1.6)$$

thereby removing m from the evolution equations while retaining it only in the constraint. In these variables the evolution system becomes

$$x' = y, \quad y' = -x - 3yz, \quad z' = x^2 - 2y^2 - z^2, \quad (1.7)$$

with constraint

$$x^2 + y^2 - z^2 = \frac{k}{m^2 a^2}. \quad (1.8)$$

This formulation underlies the classical analyses of Belinski–Grishchuk–Khalatnikov and Gibbons–Hawking–Stewart. It partitions the phase space into trajectories lying on the cone $z^2 = x^2 + y^2$ (flat models), in its interior (open models), and in its exterior (closed models), reflecting the geometry of the constraint (1.8). The dynamics is essentially hyperbolic: linearisation yields a stable focus at the origin for $k = 0$, corresponding to the late–time approach to an inflationary epoch, together with four hyperbolic equilibria at infinity representing early–time behaviour, including the big bang.

A characteristic limitation of this classical treatment is its reliance on hyperbolicity and linear stability. Eternally oscillating solutions exist but require finely tuned initial conditions. Inflation arises generically in this framework, but the picture is dominated by the stable–focus structure of the origin in the flat case and the global geometry encoded in the Friedmann constraint.

Recent observational constraints disfavour the pure quadratic potential, but polynomial extensions (notably two–parameter families) have been shown to remain compatible with all current CMB data [9, 10, 11]. The present work re-examines the foundational massive

model from the perspective of *versal unfoldings* and *mode interactions*, by replacing the above transformation with a new scaling independent of m . This introduces the single distinguished parameter $s = m^2$, and leads to a smooth one-parameter family of dynamical systems through which the transition $s > 0 \rightarrow s < 0$ (massive \leftrightarrow tachyonic) can be analysed within a unified bifurcation framework. This new formulation is developed in Section 2.

2 Summary of the main results

Dimensionless form and control parameter. To obtain a unified formulation valid for both massive ($m^2 > 0$) and tachyonic ($m^2 < 0$) scalar fields, we fix the scaling independently of m and introduce the single distinguished parameter

$$s := m^2 \in \mathbb{R}, \quad (2.1)$$

so that $s > 0$ corresponds to a convex potential, $s = 0$ to the degenerate case, and $s < 0$ to a tachyonic or hill-top potential. We then define the dimensionless variables

$$x = \frac{\phi}{\sqrt{6}}, \quad y = \frac{\dot{\phi}}{\sqrt{6}}, \quad z = H, \quad \tau = t, \quad (2.2)$$

so that a prime denotes differentiation with respect to τ . In these variables, the Einstein–scalar field equations (1.3)–(1.4) reduce to the single compact system

$$x' = y, \quad y' = -s x - 3yz, \quad z' = sx^2 - 2y^2 - z^2, \quad (2.3)$$

together with the constraint (1.5), now written as

$$sx^2 + y^2 - z^2 = \frac{k}{a^2}. \quad (2.4)$$

This form is smooth in the single real parameter s and allows a unified bifurcation analysis around the degenerate value $s = 0$, which marks the transition from oscillatory ($s > 0$) to unstable ($s < 0$) scalar–field dynamics.

Linear structure and degeneracy. For the specific value $s = 1$, the linear part of system (2.3) at the origin is equivalent to the matrix

$$\begin{pmatrix} 0 & -\omega & 0 \\ \omega & 0 & 0 \\ 0 & 0 & 0 \end{pmatrix}, \quad (2.5)$$

so that the equilibrium at the origin has one zero and two purely imaginary eigenvalues $\pm i\omega$. This simultaneous presence of a zero and a pair of imaginary eigenvalues produces a *Hopf-steady-state interaction*, the fundamental nonlinear mechanism underlying the mode interactions analyzed in this paper. The eigenvalue crossing at $s = 0$ triggers a qualitative change in stability and produces a three-dimensional centre manifold on which all local dynamics unfold.

Versal unfolding and reduced systems. Carrying out the standard normal-form analysis (following Refs. [16, 17, 18, 19, 20] and using the Fredholm alternative as in [5]), the reduced system on the centre manifold is conveniently expressed in cylindrical coordinates (r, θ, z) and takes the versal form

$$\dot{z} = \mu_1 + z^2 + d r^2, \quad \dot{r} = \mu_2 r + \frac{3}{2} r z, \quad \dot{\theta} = \omega + c_1 z, \quad (2.6)$$

where $d = \pm 1$ distinguishes the two main cases: $d = +1$ for $s > 2$ (quadratic reduction sufficient), and $d = -1$ for $s < 2$ (cubic terms required). The two unfolding parameters μ_1, μ_2 encode the leading perturbations of the degenerate linear part. Here (r, θ, z) are *state-space* coordinates (Hopf amplitude, phase and slow background variable) for the equilibrium at the origin, whereas μ_1, μ_2 denote *external* physical parameters (e.g. Taylor coefficients of $V(\phi)$). To remain within the validity of the centre-manifold reduction, one must restrict to a neighbourhood

$$|x|, |y|, |z| \leq \varepsilon, \quad |s| \leq c \varepsilon, \quad (2.7)$$

with $0 < \varepsilon \ll 1$ and $c = O(1)$. Here s has been shifted so that the organising-centre value of the original parameter (the massless threshold $s = 1$) corresponds to $s = 0$;

in these rescaled variables the limit $s \rightarrow 0$ captures the degenerate Hopf–steady–state case. This ensures that the $O(\varepsilon^2)$ terms in the vector field are of comparable magnitude and that the degenerate limit $s \rightarrow 0$ is captured correctly. Within this neighbourhood, the versal unfoldings (3.7)–(3.8) provide a complete description of the local dynamics and its physical consequences. Eliminating the rotational variable θ yields two effective two–dimensional versal families:

$$\text{Case I } (d = +1): \quad \dot{z} = \mu_1 + z^2 + r^2, \quad \dot{r} = \mu_2 r + \frac{3}{2}rz; \quad (2.8)$$

$$\text{Case II } (d = -1): \quad \dot{z} = \mu_1 + z^2 - r^2, \quad \dot{r} = \mu_2 r + \frac{3}{2}rz + \ell z^3, \quad (2.9)$$

with ℓ a constant determined by the third–order terms. Setting $\mu_1 = \mu_2 = 0$ produces the organizing centres that generate the full stratified bifurcation structure shown in Fig. 1.

Bifurcation diagrams and invariant sets. The resulting bifurcation diagrams are shown in Fig. 1 and their physical interpretation in terms of slow–roll parameters is discussed in Sect. 44.3. They consist of seven strata in Case I and eleven in Case II (see Fig. 1), corresponding to topologically distinct phase portraits organised by the versal unfolding. A key feature is the emergence and persistence of invariant tori in Case II, a direct nonlinear manifestation of Hopf–steady–state mode interaction in the full three–dimensional system (2.3). These tori arise from the limit cycles along the α –stratum of the bifurcation diagram and signal the presence of mixed geometry–matter oscillatory dynamics not detected by classical hyperbolic or linearised analyses.

How to read the bifurcation diagrams. For physical interpretation it is useful to state how slow–roll (SR), ultra slow–roll (USR) and oscillatory regimes appear in the diagrams of Fig. 1. On the centre manifold, the asymptotically stable invariant set in a given stratum determines the regime: a single hyperbolic stable equilibrium corresponds to a slow–roll attractor, while a stable limit cycle (on the α –stratum of Case II) yields a persistently oscillatory state and, in the full three–dimensional system, an invariant torus. In terms of the unfolding coordinates we have $\epsilon \sim \frac{3}{2}r^2$ and $\eta \sim z$, so hyperbolic strata

with a unique stable focus at small (r, z) (such as the χ -region in Case II) reproduce the standard SR fixed point in the $(\phi, \dot{\phi})$ -plane, whereas the γ -stratum (containing the origin) together with its neighbouring η -stratum around $(\mu_1, \mu_2) = (0, 0)$ represent the nonhyperbolic USR organising centre with $\epsilon \ll 1$ and $|\eta| = O(1)$.

Along the $E\rho$ semi-axis the system admits a nonhyperbolic continuum of periodic orbits (like the undamped harmonic oscillator), a finely tuned situation destroyed by generic perturbations. On the α -stratum this degeneracy is resolved into a single hyperbolic stable limit cycle, representing a robust oscillatory phase and, in the full system, a persistent invariant torus. Typical parameter paths then realise sequences such as $\chi \rightarrow E\rho \rightarrow \alpha$, corresponding to SR \rightarrow a mixed multi-equilibrium regime on the $E\rho$ semi-axis \rightarrow a single-frequency oscillatory state generated by the limit cycle, or $\eta \rightarrow \alpha$, corresponding to USR \rightarrow oscillatory dynamics. In this way the transitions SR \leftrightarrow USR \leftrightarrow oscillatory regimes in scalar-field cosmology are seen to be organised by the stratified structure of the versal unfolding, and reversing the motion of (μ_1, μ_2) along a path simply inverts the corresponding physical sequence (e.g. $\alpha \rightarrow E\rho \rightarrow \chi$ or $\alpha \rightarrow \eta$).

A further distinctive feature of Case II is the presence of the blow-up curve ν . As one traverses small loops in the unfolding plane around the organising-centre point, the stable limit cycle on the α -stratum grows in amplitude and eventually reaches the boundary of the local region of validity of the centre-manifold reduction along ν , realising a cycle blow-up in the sense of Ref. [18]. This curve thus mediates the transition between small-amplitude oscillations and large excursions in (r, z) within the versal unfolding.

3 The versal family: Dynamics and bifurcations

3.1 The normal form and versal unfolding

We now analyse the local dynamics of the system (2.3) near the origin for the distinguished parameter value $s = 1$. As noted in Section 2, the equilibrium at $(x, y, z) = (0, 0, 0)$ has a degenerate linear part consisting of one zero and two purely imaginary eigenvalues.

This configuration is neither hyperbolic nor reducible to a standard centre–saddle form; instead it represents a *Hopf–steady–state* mode interaction in which two oscillatory modes and one slow mode become simultaneously neutral. In this subsection we derive the associated normal form and its versal unfolding.

Rewriting the system. To place (2.3) into the canonical form used in normal–form theory, it is convenient to interchange $x \leftrightarrow y$ and rewrite the oscillatory part as

$$y'' + s y = 0,$$

so that the linear oscillations take the standard form. Introducing $x = y'$, and denoting by f, g, h the nonlinearities, the system becomes

$$x' = -s y + f(x, y, z), \quad y' = x + g(x, y, z), \quad z' = h(x, y, z), \quad (3.1)$$

where, from (2.3),

$$f = -3xz, \quad g = 0, \quad h = s y^2 - 2x^2 - z^2, \quad (3.2)$$

together with the constraint

$$x^2 + s y^2 - z^2 = \frac{k}{a^2}. \quad (3.3)$$

Reduction to the centre manifold. Following the standard procedure (cf. Refs. [16]–[20]), we shift the parameter to the origin $\mu_0 = s - 1$, identify a basis of generalized and adjoint eigenvectors of the linear part, and apply the Fredholm alternative as in [5]. This yields a three–dimensional centre manifold parametrised by (r, θ, z) in cylindrical coordinates, capturing all small perturbations of the degenerate equilibrium.

Truncating to second order, the reduced dynamics on the centre manifold takes the form

$$z' = b_1 r^2 + b_2 z^2 + O(3), \quad r' = a_1 r z + O(3), \quad \theta' = 1 + c_1 z + O(2), \quad (3.4)$$

where explicit calculation using [21] yields

$$a_1 = -\frac{3}{2}, \quad b_1 = -\frac{\mu_0 + 3}{2}, \quad b_2 = -1, \quad c_1 = 0. \quad (3.5)$$

Normalisation. A final rescaling (following the conventions in [17]) introduces the sign

$$b = \frac{-b_1 b_2}{|b_1 b_2|} = \begin{cases} +1, & s < 2, \\ -1, & s > 2, \end{cases}$$

and rewrites the normal form compactly as

$$z' = br^2 - z^2, \quad r' = -\frac{3}{2}rz. \quad (3.6)$$

Introducing $T = -\tau$ (so that \cdot now denotes differentiation with respect to T) places (3.6) into the standard form used for the two versal cases below.

3.2 Versal unfoldings and bifurcation structure

Adding the two unfolding parameters μ_1, μ_2 and including the cubic term needed when $b = +1$ yields the versal families:

Case I ($s > 2$, quadratic truncation sufficient).

$$\dot{z} = \mu_1 + z^2 + r^2, \quad \dot{r} = \mu_2 r + \frac{3}{2}rz. \quad (3.7)$$

Case II ($s < 2$, cubic term required).

$$\dot{z} = \mu_1 + z^2 - r^2, \quad \dot{r} = \mu_2 r + \frac{3}{2}rz + \ell z^3, \quad (3.8)$$

where ℓ is a nonzero constant determined by the coefficient of the cubic term in the centre–manifold reduction; its explicit value is not needed in what follows.

Both (3.7) and (3.8) are *versal unfoldings* of the degenerate organizing centre (3.6): all sufficiently small perturbations of (2.3) near $s = 1$ are locally equivalent to one of these two families.

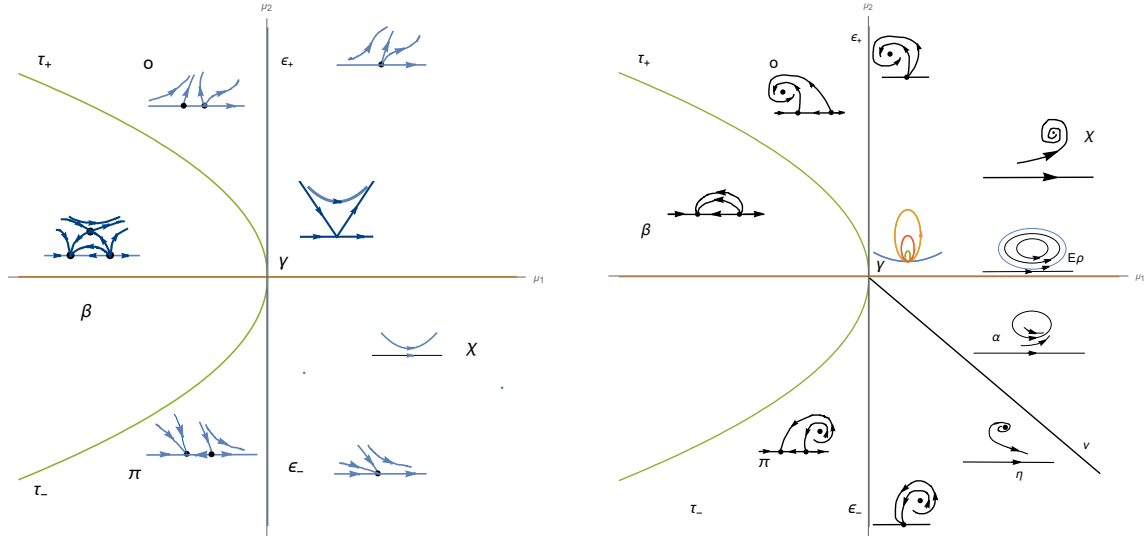


Figure 1: Bifurcation diagrams for the versally unfolded FRW–scalar field system. **Left:** The quadratic Case I ($s > 2$), exhibiting seven strata $\chi, \gamma, \varepsilon, o, \pi, \tau, \beta$. **Right:** The cubic Case II ($s < 2$), with eleven strata $\chi, \gamma, E_\rho, \alpha, \nu, \eta, \varepsilon, o, \pi, \tau, \beta$. Each stratum corresponds to a region in the unfolding parameter plane (μ_1, μ_2) with a topologically distinct phase portrait. The diagrams illustrate the organisation of saddle–node, pitchfork, and Hopf bifurcations that arise from the Hopf–steady–state mode interaction of the FRW–scalar field system.

3.3 Structure of the bifurcation diagrams

The bifurcation diagrams associated with (3.7) and (3.8) are shown in Fig. 1. In Case I there are seven strata, while in Case II there are eleven; each stratum corresponds to a region in the parameter plane (μ_1, μ_2) where the phase portrait of the system is topologically equivalent.

A useful set of first integrals of the centre-manifold dynamics at both organising centres (i.e. for $\mu_1 = \mu_2 = 0$) is given by

$$I_n(z, r) = \frac{n}{2} r^{2/n} (z^2 \pm r^2)^{1-n}, \quad (3.9)$$

with $n = \frac{3}{2}$ and the upper sign for Case I, the lower for Case II. For these organising-centre

systems the integrals provide a complete description of the orbits in a neighbourhood of the equilibrium and recover, as special cases, the stable-focus behaviour of the flat FRW model found in Refs. [13, 14].

An important nonlinear feature of the Case II unfolding is the phenomenon of cycle blow-up in the sense of Kuznetsov [18]. Along parameter loops encircling the organising-centre point, a small limit cycle born in a Hopf bifurcation on the α -stratum can grow and reach the boundary of any fixed neighbourhood of the origin before disappearing from the local centre-manifold description along the curve ν (the analogue of Kuznetsov's J -curve). Cosmologically this means that arbitrarily small deformations of the effective parameters (μ_1, μ_2) at the organising centre (corresponding to the massless transition) can drive the coupled scalar-geometry oscillations from negligible amplitude to order-one excursions in (r, z) , sharply amplifying the sensitivity of post-inflationary dynamics to microphysical details of the potential.

3.4 Fixed branches and bifurcations

The two versal families admit up to three fixed branches in a neighbourhood of $(\mu_1, \mu_2) = (0, 0)$ that unfold the Milne equilibrium of the FRW system. For both cases, the primary branches are

$$E_{1,2} = (z_{1,2}^{(0)}, 0) = (\mp\sqrt{-\mu_1}, 0), \quad (3.10)$$

which exist for $\mu_1 < 0$. A third branch appears in each case:

Case I.

$$Z_I = \left(-\frac{\mu_2}{n}, \sqrt{-\frac{\mu_2^2}{n^2} - \mu_1} \right), \quad \text{real when } \mu_1 < -\frac{\mu_2^2}{n^2}. \quad (3.11)$$

Case II.

$$Z_{II} = \left(-\frac{\mu_2}{n}, \sqrt{\frac{\mu_2^2}{n^2} + \mu_1} \right), \quad \text{real when } \mu_2^2/n^2 + \mu_1 > 0. \quad (3.12)$$

The stability and bifurcation properties of these branches follow directly from the linearisation and have been extensively analysed in [7]. We summarise the results here:

Theorem 3.1 (Stability of the fixed branches) *The equilibria $E_{1,2}, Z_I, Z_{II}$ exhibit the following behaviour:*

1. E_1 is a saddle, sink, or bifurcates when $\mu_2 - n\sqrt{-\mu_1}$ is > 0 , < 0 , or $= 0$, respectively.
2. E_2 is a source, saddle, or bifurcates when $\mu_2 + n\sqrt{-\mu_1}$ is > 0 , < 0 , or $= 0$, respectively.
3. Z_I is always a saddle (Case I) and limits to E_1 or E_2 depending on whether the τ^+ or τ^- branch is followed.
4. Z_{II} (Case II) exhibits:
 - (a) real eigenvalues: source for $\mu_2 < 0$, sink for $\mu_2 > 0$;
 - (b) complex eigenvalues: unstable node if $\mu_2 < 0$, stable node if $\mu_2 > 0$;
 - (c) purely imaginary eigenvalues at $\mu_2 = 0, \mu_1 > 0$: a degenerate Hopf bifurcation producing an infinite family of closed orbits, stabilised by cubic terms.

Geometric interpretation. Crossing the various strata induces three characteristic bifurcations:

- *Saddle-node (horizontal, z -direction):* creation or annihilation of $E_{1,2}$.
- *Pitchfork (vertical, r -direction):* appearance of the branch Z_I in Case I.
- *Hopf and torus formation (diagonal directions):* in Case II, the branch Z_{II} undergoes a Hopf bifurcation, creating a limit cycle which lifts to an invariant torus of the full three-dimensional system.

These bifurcations account for the geometry of the strata shown in Fig. 1 and underlie the coupled scalar-field and geometric oscillations generated by the Hopf-steady-state interaction, whose detailed behaviour is analysed below.

4 Physical implications of the versal unfolding

The bifurcation diagrams obtained in the previous section summarise the local phase–space organisation of the Einstein–scalar flow near the Hopf–steady–state organising centre at $s = 1$. Each stratum of the versal unfolding corresponds to a distinct dynamical regime, characterised by specific configurations of equilibria, periodic orbits, and—in the cubic case— invariant tori. These structures determine the qualitative behaviour of cosmological solutions in a neighbourhood of the degeneracy, and their arrangement in the unfolding plane provides a geometric framework for understanding the various possible evolutionary paths of FRW scalar–field universes.

In this section we outline the physical interpretation of these regimes. We begin by describing the dynamical significance of the fixed branches and invariant sets, then discuss how the mode interaction constrains the behaviour of the Hubble variable and the scalar field. We finally show how the observable quantities (n_s, r_s, A_s) emerge directly from the unfolding variables (z, r) , providing a geometric explanation for the robustness of inflationary behaviour.

4.1 Interpretation of the strata

Interpretation. The physical meaning of the dynamical structures in the versal unfolding is most transparent when discussed separately for the two organising families.

Case I (quadratic family). In this regime the fixed branches $E_{1,2}$ and the parabolic curve Z_I govern the evolution near the organising centre. The dynamics is dominated by the competition between the slow geometric mode z and the scalar oscillation amplitude r , with no higher–order geometric feedback. Trajectories typically approach one of the fixed branches, corresponding either to slow contraction ($z < 0$), slow expansion ($z > 0$), or near–critical evolution along the fold of the parabola. The absence of cubic terms suppresses the formation of secondary oscillatory structures: no invariant tori occur in this family. Cosmologically, Case I represents universes whose dynamics is controlled by

a single dominant mode (expanding or contracting) with weak scalar–field interaction, producing monotonic or weakly damped behaviour of the Hubble rate.

Case II (cubic family). The cubic term in the r –equation induces a qualitatively richer set of dynamical behaviours. In addition to the fixed branches $E_{1,2}$, the cubic family contains the *cusp*–shaped curve Z_{II} and supports the emergence of invariant tori through a secondary Hopf mechanism. These tori correspond to persistent coupled oscillations of the geometric mode z and the scalar–field oscillation amplitude r , representing sustained geometry–matter interactions. Such mixed oscillatory states do not appear in Case I. Cosmologically, Case II therefore describes universes in which the scalar and geometric modes remain dynamically entangled for long periods, producing quasi–periodic evolution of the Hubble parameter and the scalar energy density. This richer oscillatory behaviour is a signature of the cubic unfolding and is structurally stable within its domain.

In both cases the neighbourhood of $s = 1$ forces the system into regimes with small r and small z , yielding the universal slow–roll expressions derived below. Thus the geometric origin of near–inflationary evolution holds across both versal families, despite their very different phase–space structures. It is important to note that the physically realised Einstein–scalar system lies on the cubic side of the unfolding. In a neighbourhood of $s = 1$, the normal-form coefficient determining the sign of the unfolding is negative, so that the dynamics unfolds within the Case II family. This explains why invariant tori and mixed scalar–geometric oscillations are generic in the physical problem. Moreover, the massless case $s = 0$ may be viewed as lying on a lower-dimensional degenerate subset of this unfolding: when the x –dependence is suppressed at $s = 1$, the resulting flow reproduces the qualitative structure of the massless system. Thus the $s = 0$ dynamics is naturally embedded in the geometry of the organising centre at $s = 1$.

4.2 Implications for the full three-dimensional system

Although the reductions (3.7)–(3.8) are two-dimensional, their bifurcation structures lift to the full three-dimensional system (3.4), where the equilibria $E_{1,2}$ correspond to

equilibrium *points*, the nontrivial fixed branch Z_I corresponds to a limit cycle of the same stability, and the limit cycle in (r, z) corresponds to an invariant torus. In particular:

- The saddle-node creation of $E_{1,2}$ corresponds to changes in the qualitative behaviour of H and $\dot{\phi}$, determining whether the model is attracted to inflationary expansion or diverges away from it.
- The pitchfork birth of Z_I marks a transition from geometry-dominated to matter-dominated behaviour on the centre manifold, shifting the equilibrium among curvature, kinetic, and potential terms.
- The Hopf bifurcation of Z_{II} produces a limit cycle in the reduced system, which lifts to an *invariant torus* in the full system, signalling the onset of sustained quasi-periodic oscillations in $(\phi, \dot{\phi}, H)$.

These effects are invisible to purely linearised analyses and arise only through a fully nonlinear treatment of the degeneracy at $s = 1$.

In the cubic unfolding (Case II), the periodic orbit on the (z, r) -plane lifts to a two-torus when rotated along the Hopf phase θ . This is the standard mechanism illustrated in various references (e.g., [17, 18]): a periodic orbit in the reduced system (z, r) generates an invariant torus $S^1 \times S^1$ in the full three-dimensional flow.

Cosmologically, such tori correspond to persistent quasi-periodic oscillations of both the scalar-field kinetic energy and the Hubble parameter. The universe undergoes long-lived, non-chaotic oscillations in which the scalar and geometric modes remain dynamically coupled, resulting in a continuous, modulated exchange of energy between matter and geometry. These quasi-periodic states arise purely from the geometric structure of the organising centre and do not require any oscillatory features in the potential. They may be interpreted as structurally stable pre- or post-inflationary phases with sustained scalar-geometry interactions.

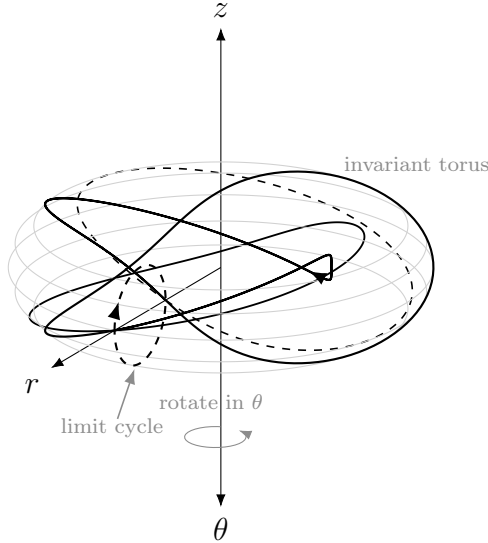


Figure 2: Lifting of a periodic orbit to an invariant torus in the Hopf–steady–state interaction. A limit cycle in the reduced (r, z) dynamics (dashed curve where the torus is cut by the (r, z) -plane) is rotated along the Hopf phase θ , producing an invariant two-torus $S^1 \times S^1$ in the full (r, z, θ) flow. The solid winding curve illustrates a typical quasi-periodic orbit on the torus, corresponding to persistent coupled oscillations of the Hubble mode z and the scalar oscillation amplitude r in Case II.

4.3 Slow-roll observables from the unfolding

From the definitions (2.2), we work with $y = \dot{\phi}/\sqrt{6}$ and $z = H$, so that for $k = 0$ the Friedmann constraint reads

$$z^2 = \frac{1}{3} \left(\frac{1}{2} \dot{\phi}^2 + V \right) = \frac{1}{3} (3y^2 + V).$$

Along the slowly expanding branch of the centre manifold we have $y = O(r)$ and $V(\phi) = V(\phi_0) + O(r^2)$, hence $z^2 = \frac{1}{3} V(\phi_0) + O(r^2)$. In the scaled variables used here this gives

$$z^2 = \frac{1}{3} + O(\mu_1, \mu_2, r^2), \quad (4.1)$$

which is precisely the *organising-centre background ansatz* at the origin: for the bifurcation value of the parameters the equilibrium becomes nonhyperbolic of Hopf–steady–state

type. Thus the slowly expanding branch of the centre manifold is anchored at a de Sitter state with $z^2 \simeq V(\phi_0)/3$, and at this parameter value the equilibrium at the origin is a nonhyperbolic Hopf–steady–state point, i.e. the codimension-two organising centre whose versal unfolding is given by (2.8)–(2.9).

From the dynamical-systems viewpoint slow–roll (SR) and ultra slow–roll (USR) admit a simple qualitative characterisation on the centre manifold. In strata such as χ the origin is a hyperbolic stable focus and the late-time behaviour of generic initial data in its basin is SR: the background trajectory spirals into the focus with small (r, z) and the associated slow-roll parameters satisfy $\epsilon \ll 1, |\eta| \ll 1$. Here ϵ is the first Hubble slow-roll parameter and η is essentially the second Hubble slow-roll parameter (often denoted ϵ_2), rather than the potential parameter $\eta_V \propto V''/V$. In contrast, at the organising-centre point γ and along its hyperbolic continuation in the η –stratum the origin represents a non-attractor background: it is either nonhyperbolic (at γ) or a weakly unstable focus (in η), so trajectories that pass close to the origin experience a finite USR episode, with $\epsilon \ll 1$ but $|\eta| = O(1)$, before peeling off towards other equilibria or oscillatory states. In this sense SR corresponds to a genuine hyperbolic attractor, whereas USR appears as a transient passage near the non-attractor organising centre and its unstable continuation.

From the perturbation point of view, this USR window corresponds to the usual non–attractor ultra slow–roll phase, in which the comoving curvature perturbation acquires a growing mode and the scalar power spectrum increases; in phenomenological applications this is precisely the type of phase typically invoked for primordial black–hole production.

The Hopf amplitude r measures the small kinetic departure from de Sitter, and the fast phase θ averages out at leading order. Since $H = z$ in our normalisation, the exact identity for the first slow-roll parameter,

$$\epsilon(\tau) = -\frac{\dot{H}}{H^2}, \quad (4.2)$$

becomes, using Eq. (4.1), $\dot{\phi}^2 = 6y^2$, and $y^2 = \frac{1}{2}r^2 + O(r^3)$,

$$\epsilon = \frac{3y^2}{z^2} = \frac{3}{2}r^2 + O(\mu_1, \mu_2, r^4), \quad (4.3)$$

so the first slow-roll parameter is directly proportional to the square of the Hopf amplitude:

$$\epsilon \sim \frac{3}{2}r^2. \quad (4.4)$$

For the second slow-roll parameter,

$$\eta(\tau) = \frac{\dot{\epsilon}}{H\epsilon}, \quad (4.5)$$

we use $r' = -\frac{3}{2}rz$ from the organising-centre equations. This gives

$$\frac{\dot{\epsilon}}{\epsilon} = \frac{d}{d\tau}(\ln r^2) = -3z, \quad (4.6)$$

and hence

$$\eta = \frac{-3z}{z} = -3. \quad (4.7)$$

Therefore at the organising centre the exact Hubble parameter η takes the background value $\eta = -3$, originating from the geometric friction term $3H\dot{\phi}$. This constant corresponds to the de Sitter decay rate and can be absorbed into the normal-form normalisation: we consider instead the slow residual part $\eta_{\text{slow}} := \eta + 3$, whose leading contribution is linear in the geometric mode z . After this normalisation and the averaging over the fast Hopf phase already used in the derivation of $\epsilon \simeq \frac{3}{2}r^2$, we obtain,

$$\eta_{\text{slow}} \sim z. \quad (4.8)$$

To avoid extra notation we continue to denote η_{slow} simply by η in what follows.

To leading order, all inflationary observables depend only on the unfolding variables (r, z) :

$$n_s \approx 1 - 6\epsilon + 2\eta, \quad r_s \approx 16\epsilon, \quad A_s \approx \frac{H^2}{8\pi^2\epsilon}, \quad (4.9)$$

which using (4.4)–(4.8) become

$$n_s \approx 1 - 9r^2 + 2z, \quad r_s \approx 24r^2, \quad A_s \approx \frac{z^2}{12\pi^2r^2}. \quad (4.10)$$

These formulae constitute a universal prediction of the unfolding: the observed spectral tilt and tensor amplitude depend only on the small kinetic and geometric modes (r, z) of the organising centre, independently of any assumed potential.

4.3.1 Physical meaning of the unfolding parameters

The unfolding parameters (μ_1, μ_2) describe all small deformations of the organising centre $s = 1$. Physically, they correspond to the two independent ways in which the effective inflationary dynamics can deviate from the quadratic model: μ_1 produces a shift/tilt deformation (breaking the $\phi \mapsto -\phi$ symmetry and changing the relative strengths of the slow modes), and μ_2 controls the curvature and plateau behaviour of the effective dynamics at large field values. In particle-physics models, these deformations typically appear as parameters in the inflaton potential. For example, the polynomial potential [10, 11],

$$V(\phi) = \frac{1}{2}m^2\phi^2(1 - a\phi + b(a\phi)^2)^2, \quad (4.11)$$

has deformation parameters (a, b) playing exactly the roles of (μ_1, μ_2) : a induces a tilt and b controls the asymptotic flattening. Our unfolding therefore provides a universal, potential-independent classification of all such deformations. In particular, the observables (4.10) depend only on the unfolding variables (r, z) and the geometric parameters (μ_1, μ_2) , and not on any specific choice of potential.

5 Discussion

The analysis developed in this paper shows that the dynamics of spatially homogeneous scalar-field cosmology near the massless transition $s = 1$ is governed by a codimension-two organising centre of Hopf-steady-state type. The versal unfolding of this centre captures *all* small deformations of the quadratic model, independently of the choice of potential. The centre manifold contains two slow geometric modes (r, z) , where r measures the small kinetic departure from de Sitter and z is the slow drift of the Hubble mode. All other degrees of freedom are either fast (the Hopf phase θ) or slaved by the constraint. This reduction is universal: any scalar potential with a nondegenerate minimum and regular polynomial large-field behaviour induces only a reparametrisation of the unfolding parameters (μ_1, μ_2) .

A key conclusion is that the inflationary observables (n_s, r_s, A_s) arise directly from the dynamics of the unfolding. The first slow-roll parameter is proportional to the square of the Hopf amplitude, $\epsilon \simeq \frac{3}{2}r^2$, while the second is the slow geometric mode itself, $\eta \simeq z$. Consequently, the spectral tilt, the tensor-to-scalar ratio, and the scalar amplitude from Eq. (4.10) are determined solely by the unfolding variables (r, z) and the geometric parameters (μ_1, μ_2) , with no reference to an underlying potential. This identification is conceptually significant: the near scale-invariance of primordial perturbations emerges as a *geometric property* of the organising centre, not as a feature requiring any specific inflaton Lagrangian.

In particular, the familiar inflationary sequence of a slow-roll phase, possible ultra slow-roll interludes, and a final oscillatory regime appears here as a stratified bifurcation scenario. On the centre manifold, SR corresponds to hyperbolic strata such as χ with a unique stable focus, USR to the organising-centre point γ and its unstable continuation in the η -stratum, and the oscillatory phase to the stable limit cycle on the α -stratum (lifting to an invariant torus in the full flow). The Case II bifurcation diagram therefore encodes the allowed transitions between SR, USR and oscillatory behaviour, while the underlying microphysics selects a particular path in this stratified geometry. Our analysis is local in phase space and parameter space around the organising centre and does not by itself determine the global end of inflation or the total number of e-folds; these depend on how the trajectory exits the neighbourhood of the unfolding and on additional physics (e.g. reheating).

It is instructive to compare this with the potential-based approach. In the models of [10, 11], the potential contains two deformation parameters (a, b) , which control the tilt and the large-field curvature of the potential. These parameters play exactly the roles of the unfolding variables (μ_1, μ_2) in our setting: a generates a shift/tilt deformation breaking the $\phi \mapsto -\phi$ symmetry, and b governs the deformation of the large-field behaviour away from the purely quadratic model. The mapping is structural: the space of potentials realising small deformations of the quadratic model corresponds to a two-dimensional surface in the (μ_1, μ_2) -plane. Our unfolding therefore provides a *potential-independent*

and *canonically normalised* description of all such models.

The geometric picture that emerges is that inflation itself is a structurally stable phenomenon associated with the unfolding of the organising centre. The slow variation of (r, z) along the expanding branch of the centre manifold forces $\epsilon \ll 1, \eta \ll 1$, and hence predicts a nearly scale-invariant spectrum of perturbations. In this sense, the familiar inflationary predictions arise here as a dynamical consequence of the unfolding geometry. If inflationary theory did not exist, the universal behaviour encoded in the versal unfolding of the massive scalar-field system would provide a natural mechanism for an early phase of accelerated expansion with precisely the observed form of primordial perturbations.

This viewpoint suggests a broader interpretation: the space of inflationary models is not a set of disparate potentials but a low-dimensional geometric manifold parametrised by the unfolding coordinates (μ_1, μ_2) . The role of any specific potential is simply to select a path in this space. From this perspective the relations (4.10) are universal predictions of massive scalar-field cosmology, valid for any model lying sufficiently close to the organising centre (i.e. belonging to the ‘versal envelope’ of the massive scalar field). The unfolding thus provides a unifying framework for the observational phenomenology of inflaton models, independent of their microscopic origin. Moreover, the same versal structure organises not only slow-roll attractors but also ultra slow-roll transients and oscillatory torus phases, as seen in the stratified Case II diagram.

Finally, the existence of this organising centre and its unfolding hints at the possibility of a more global bifurcation structure in cosmology. As in other areas of dynamics, the classification of neighbourhoods of singular points often extends to more global structures, and it would be interesting to investigate whether the scalar-field dynamics admits further degeneracies or mode interactions beyond the Hopf-steady-state considered here. These questions lie at the interface of bifurcation theory, cosmology, and the theory of early-time perturbations, and point toward a more geometric understanding of inflation.

Acknowledgments

The research of SC was funded by RUDN University, scientific project number FSSF-2023-0003. The work of IA was supported in part by the Second Century Fund (C2F), Chulalongkorn University.

References

- [1] A. H. Guth, *The Inflationary Universe: A Possible Solution to the Horizon and Flatness Problems*, Phys. Rev. D23 (1981) 347.
- [2] A.D. Linde, *Chaotic Inflation*, Phys. Lett. B129 (1983) 177.
- [3] V. Mukhanov, *Physical Foundations of Cosmology* (CUP, Cambridge, 2005)
- [4] S. Cotsakis, *Structural stability and general relativity*, Universe 11(7) (2025) 209; arXiv:2412.04283.
- [5] S. Cotsakis, *Friedmann–Lemaître universes and their metamorphoses*, Eur. Phys. J. C 85 (2025) 579; arXiv:2411.17286.
- [6] S. Cotsakis, *The crease flow on null hypersurfaces*, Eur. Phys. J. C 84 (2024) 391; arXiv:2312.08023.
- [7] S. Cotsakis, *Bifurcation diagrams for spacetime singularities and black holes*, Eur. Phys. J. C 84 (2024) 35; arXiv:2311.16000.
- [8] S. Cotsakis, *Dispersive Friedmann universes and synchronization*, Gen. Relativ. Gravit. 55 (2023) 61; arXiv:2208.07892.
- [9] BICEP, Keck collaboration, *Improved Constraints on Primordial Gravitational Waves using Planck, WMAP, and BICEP/Keck Observations through the 2018 Observing Season*, Phys. Rev. Lett. 127 (2021) 151301 [2110.00483].

- [10] R. Kallosh, A. Linde and A. Westphal, *Chaotic Inflation in Supergravity after Planck and BICEP2*, Phys. Rev. D90 (2014) 023534 arXiv:1405.0270.
- [11] R. Kallosh, A. Linde, *On the present status of inflationary cosmology*, Gen. Rel. Grav. 57 (2025) 10, 135; arXiv:2505.13646 [hep-th]
- [12] V. A. Belinski, L. P. Grishchuk, I. M. Khalatnikov, and Ya. B. Zel'dovich, *Inflationary stages in cosmological models with a scalar field*, Phys. Lett. B **155B** (1985) 232.
- [13] V. A. Belinski, L. P. Grishchuk, Ya. B. Zel'dovich, and I. M. Khalatnikov, *Inflationary stages in cosmological models with a scalar field*, Sov. Phys. JETP **62** (1985) 195.
- [14] G. W. Gibbons, S. W. Hawking, and J. M. Stewart, *A Natural Measure on the Set of All Universes*, Nucl. Phys. B **281** (1987) 736.
- [15] V. A. Belinski, H. Ishihara, I. M. Khalatnikov, and H. Sato, *On the degree of generality of inflation in Friedmann cosmological models with a massive scalar field*, Prog. Theor. Phys. 79 (1988) 676.
- [16] M. Golubitsky, I. Stewart, D. G. Schaeffer, *Singularities and Groups in Bifurcation Theory*, Volume II (Springer, 1988)
- [17] S. Wiggins, *Introduction to applied nonlinear dynamical systems and chaos*, 2nd. Ed. (Springer, 2003)
- [18] Yu. A. Kuznetsov, *Elements of Applied Bifurcation Theory*, Fourth Ed. (Springer, AMS 112, 2023)
- [19] J. Guckenheimer and P. Holmes, *Nonlinear oscillations, dynamical systems, and bifurcations of vector fields* (Springer, 1983)
- [20] V. I. Arnold, *Dynamical Systems V: Bifurcation Theory and Catastrophe Theory* (Springer, 1994)
- [21] R. W. Wittenberg and P. Holmes, Physica D**100** (1997) 1-40